

Molecular Dynamics Insight into the Urea Effect on Tretinoin Encapsulation into Carbon Nanotube

Maryam Ghadamgahi^a and Davood Ajloo^{*,a,b}

^aSchool of Chemistry, Damghan University, 3671641167 Damghan, Iran

^bDepartment of Physical Chemistry, School of Chemistry, College of Science, University of Tehran, 141556455 Tehran, Iran

Simulações moleculares dinâmicas a 270 e 310 K racionalizam o efeito da ureia, temperatura e tamanho dos nanotubos de carbono, na inserção de Tretinoin em nanotubos com quiralidade (10, 7) e (8, 5). Concentrações de 0,9 mmol L⁻¹ e 2 mol L⁻¹ de ureia foram estudadas, sendo menor e maior que a faixa normal de ureia no sangue, respectivamente. Os resultados mostram que o encapsulamento de Tretinoin pode ser atribuído ao fluxo de água via interações hidrofílicas e de van der Waals, e ao diâmetro do nanotubo. Capacidade calorífica, coeficiente de difusão, energia livre e coeficiente de contato mudam com a temperatura e ureia. A molécula de Tretinoin localiza-se dentro do nanotubo devido às interações parciais π - π entre o átomo de oxigênio e os anéis aromáticos conjugados do nanotubo. A alta concentração de ureia causa o impressionante fenômeno de induzir a secagem do nanotubo, resultando em fios de ureia e instabilidade do encapsulamento.

Molecular dynamics simulations at 270 and 310 K rationalized the effect of urea, temperature and the size of the carbon nanotube, on the insertion of Tretinoin into nanotubes with chirality (10, 7) and (8, 5). Concentrations of 0.9 mmol L⁻¹ and 2 mol L⁻¹ of urea are studied, that are less and more than the normal range of blood urea content, respectively. Results show that encapsulation of Tretinoin could be ascribed to the flow of the waters via hydrophilic and van der Waals interactions and diameter of the nanotube. Heat capacity, diffusion coefficient, free energy and contact coefficient change with the temperature and urea. Tretinoin molecule locates inside the nanotube due to the partial π - π interactions between oxygen atom of Tretinoin and the conjugated aromatic rings of nanotube. Finally, high concentration of urea causes the striking phenomenon of inducing the drying of nanotube that result in urea wires and instability of encapsulation.

Keywords: carbon nanotube, molecular dynamics simulation, Tretinoin, linear interaction energy

Introduction

Reducing toxicity of therapeutic materials is the main aim of developing drug-delivery systems that is achieved using carbon nanotubes (CNTs).^{1,2} The intense interest in CNTs is due to the capability of absorbing or conjugating with a wide variety of medicinal molecules.³ They have unique chemical and physical properties and applications from high strength and low weight nanocomposite materials to electronic devices.⁴ Drug molecule penetrates through the cancer cell by CNT to treat diseases and thereby potentially reducing the drug side effects by preserving the non-cancerous tissues of the patients.⁵ This is a characteristic of

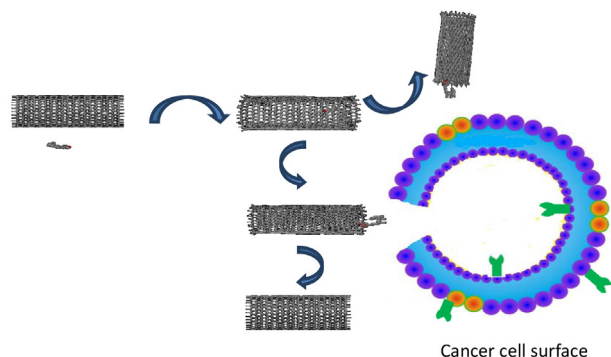
some functionalized CNT, designed to selectively direct the drug toward the cancer cells, thus overcoming one of the main limitations of the most existing anticancer therapies, namely the lack of selectivity.⁶ The delivery potential of anticancer drugs might be ascribed to their needle-like shapes, which enable them to insert into the target cancer cells after covalently bonding to drug.^{7,8}

The most common form of human cancer, skin cancer, estimates to occur over two million new cases annually.⁹ The increase of annual rates of skin cancer each year represents public concern. As a result, to treat this cancer, various methods and drugs have developed in which the drug inserts the CNT and targets the cancer cell surface.^{10,11}

Scheme 1 shows an anticancer system in which the Tretinoin agent inserts into the CNT and targets cancer

*e-mail: ajloo@du.ac.ir, ajloo@ut.ac.ir

cell surface, a “longboat” cancer system developed by Dhar *et al.*¹²



Scheme 1. Schematic representation of inserted Tretinoin into the CNT, targeting cancer cell surface.¹²

The interaction and insertion of drug molecules inside CNT has been mainly driven by the van der Waals interaction between species¹³⁻¹⁵ and it has been confirmed previously that the hydrophobic drugs can also be adsorbed into the hydrophobic CNT surface.¹⁶ Likewise, Rungrim *et al.*¹⁷ demonstrated that the π - π stacking of two cytosine rings of adjacent gemcitabine molecules cause them to orientate towards each other and move together inside the CNT.

Up to date, various theoretical studies have attempted to rationalize the drug delivery dependence on solvent environment and temperature.¹⁸⁻²¹ Dalili *et al.*²² compared interaction of an anti cancer drug and CNT in ethanol, methanol and water using semi empirical models and provided that these composites are more stable in water than other solvents.

Co-solvents such as urea can be confined inside CNT and form molecular wires. They have attracted particular interest recently, due to their scientific importance in biological channels.²³ The hydrophobic CNTs with proper diameters might serve as useful model systems to study biological urea channel. Xiu *et al.*²⁴ and Liu *et al.*²⁵ have provided that urea molecules can induce urea wires by drying of CNTs.

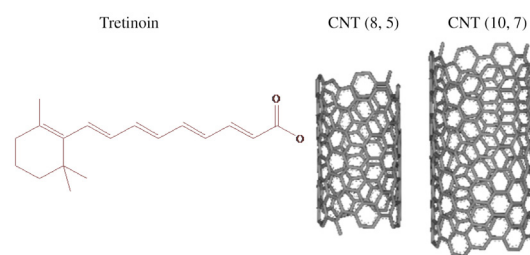
In this work, the studied anti-cancer drug is Tretinoin, that is used to treat acne and photo damaged skin and is the main regulator of cell proliferation, reproduction and differentiation.²⁶ Urea can considerably increase the release of drugs from ointment bases and that it is one of the most effective penetration promoters for topically applied drugs. On the other hand, all-*trans* retinoic acid (Tretinoin) has been already used for treatment of other cancers using different routes of administration.²⁷ This work focuses on the ability of loading Tretinoin inside a (10, 7) and (8, 5) CNT by urea. Interaction energy between the drug molecule and CNT in water and urea are analyzed and discussed at

270 and 310 K using molecular dynamics (MD) simulation. Further, the interaction and encapsulation of Tretinoin in different urea level (higher and less than blood normal range) are also focused, and linear interaction energy (LIE) method provides their free energies.

Experimental

Molecular dynamics simulation

The structure of Tretinoin and urea were drawn using HyperChem 7 software²⁸ and their final geometries were optimized with the semi-empirical AM1 method.²⁹ PRODRG2³⁰ server was used to generate force field parameters and TubeGen 3.4³¹ online servers was used to create a series of uncapped armchair carbon nanotubes with chirality of (10, 7) (with a 1.4 nm diameter and 1.9 nm length) and (8, 5) (with a 0.9 nm diameter and 1.4 nm length). The chiralities are selected according to earlier studies^{17,26} on similar drug and smallest optimized size for encapsulation. Scheme 2 displays the structure of Tretinoin and the provided nanotubes.



Scheme 2. Structure of Tretinoin and CNTs.

To set up the initial configurations, Tretinoin was placed out of CNT and separated sufficiently far away (> 3 nm) to minimize the effect of starting orientations. Tretinoin was aligned in a similar position from both CNTs. Then, the simulation box was solvated with SPC/E water model, and the charge of the system was neutralized by adding sodium and chloride ions. Since urea is solvated in cellular solutions in physiological conditions, 0.9 mmol L^{-1} and 2 mol L^{-1} urea was added to some systems to consider how the system would be affected by it. Molecular dynamics simulation was performed using GROMACS software version 4.5.4.³² To model atomic interactions, GROMOSE96 force field was applied.²⁶ The temperature was kept close to the intended values (310 and 270 K) using the Nose-Hoover algorithm. Pressure was also kept constant (1 bar) using Parrinello-Rahman algorithm.³³ Leap-Frog integration algorithm was used to solve the equation of motion by a time step of two femtoseconds. LINCS algorithm was

used to constrain all bonds, including hydrogen bonds.³³ Particle-Mesh Ewald (PME) method was used to calculate long-range electrostatic interactions while electrostatic interactions between charged groups within 1.5 nm were calculated explicitly.³⁴ Lenard-Jones (L-J) and van der Waals interactions were calculated with a 1.5 nm range cutoff. Grid algorithm was used to search neighbours.³⁵ Table 1 lists a summary of the simulations.

To relax solvent/co-solvent molecules, all systems were equilibrated by 1 ns with position restraints on the Tretinoin and CNT. After equilibration, the molecular dynamic run was 16 ns. All production runs were obtained three times to check repeatability and results were averaged from three independent trajectories.

Heat capacity

A straightforward method to calculate the heat capacity at constant pressure (C_p) is to use the enthalpy equation³⁶

$$H = E + PV \quad (1)$$

where E , V and P are the average internal energy, the average volume and the pressure of system, respectively.

$$C_p = \frac{\langle H^2 \rangle - \langle H \rangle^2}{RT^2} \quad (2)$$

$$\langle H \rangle = \frac{\sum_V \sum_i H_i e^{-E_i(V)/kT} e^{-PV/KT}}{\sum_V \sum_i e^{-E_i(V)/kT} e^{-PV/KT}} \quad (3)$$

where $\langle H \rangle$, H_i and k are the average value of enthalpy, enthalpy of i th state and Boltzmann constant respectively.^{36,37}

Diffusion coefficient

The average distance that a molecule travels over time is mean square displacement (MSD). Einstein relation of MSD was used to determine the self-diffusion coefficient D_A of particle A :

$$MSD = R(t) = \langle \|r_i(t) - r_i(0)\|^2 \rangle \quad (4)$$

$$\lim_{t \rightarrow \infty} \langle \|r_i(t) - r_i(0)\|^2 \rangle = 6D_A t \quad (5)$$

where $r_i(t) - r_i(0)$ is traveled distance by molecule i over time interval of t .³⁸

Free energy

Binding free energy was calculated using semi-empirical LIE method introduced by Aqvist *et al.*³⁹ The LIE method divides the interaction between ligand and its surrounds into electrostatic and van der Waals terms.

$$\Delta G_{\text{binding}} = \alpha \langle V_{1-s}^{\text{vdW}} \rangle_{\text{bound}} - \langle V_{1-s}^{\text{vdW}} \rangle_{\text{free}} + \beta \langle V_{1-s}^{\text{el}} \rangle_{\text{bound}} - \langle V_{1-s}^{\text{el}} \rangle_{\text{free}} + \gamma \quad (6)$$

where $\langle V_{1-s}^{\text{el}} \rangle_{\text{free}}$ and $\langle V_{1-s}^{\text{vdW}} \rangle_{\text{free}}$ are the average electrostatic and van der Waals interaction energies from an MD

Table 1. Summary of set up systems (duration of all systems was 3×16 ns)

No.	CNT	Solvent/co-solvent	No. water	Conc. co-solvent / (mmol L ⁻¹)	T / K
1	Tretinoin-CNT(8,5)	Water	4382	0	270
2	Tretinoin-CNT(8,5)		4382	0	310
3	Tretinoin-CNT(8,5)	Water/urea	4291	0.9	270
4	Tretinoin-CNT(8,5)		4291	0.9	310
5	Tretinoin-CNT(8,5)	Water/urea	4241	2000	270
6	Tretinoin-CNT(8,5)		4241	2000	310
7	Tretinoin-CNT(10,7)	Water	5271	0	270
8	Tretinoin-CNT(10,7)		5271	0	310
9	Tretinoin-CNT(10,7)	Water/urea	5172	0.9	270
10	Tretinoin-CNT(10,7)		5172	0.9	310
11	Tretinoin-CNT(10,7)	Water/urea	5120	2000	270
12	Tretinoin-CNT(10,7)		5120	2000	310
13	Tretinoin	Water	4466	0	270
14	Tretinoin		4466	0	310
15	Tretinoin	Water/urea	4375	0.9	270
16	Tretinoin		4375	0.9	310
17	Tretinoin	Water/urea	4163	2000	270
18	Tretinoin		4163	2000	310

trajectory of the ligand in water and $\langle V_{1-s}^{\text{el}} \rangle_{\text{bound}}$ and $\langle V_{1-s}^{\text{vdW}} \rangle_{\text{bound}}$ are the same average energies from another molecular dynamics trajectory with ligand bound to CNT. The angle bracket indicates Boltzmann average and the subscripts 1 and s refer to the ligand (Tretinoin) and the surround, respectively. It was found for several ligand-nanotube systems that a set of values of $\alpha = 0.5$ and $\beta = 0.16$ give results in agreement with experimental data.⁴⁰ γ is a constant term obtained by regression fitting that gives absolute binding free energies.⁴¹ The results from LIE calculations, using the earlier optimized model of Hansson *et al.*⁴² with $\gamma = 0$, give relative binding free energies that agree very well with the experimental binding data.⁴³⁻⁴⁵

Potential of mean force (PMF)

PMF between the solutes was calculated using mean square displacement that gives us a measure of the average distance a molecule travel:

$$PMF = -k_B T \ln g(r) \quad (7)$$

where k_B , T and $g(r)$ are the Boltzmann constant, simulation temperature, and radial distribution function (RDF) between the solutes, respectively.⁴⁶

Contact coefficient

The contact coefficient $C_u - C_{CNT}$ was calculated to illustrate the interaction frequency between the CNT and urea in detail:

$$C_u - C_{CNT} = \frac{N_{CNT-u} M_w}{N_{CNT-w} M_u} \quad (8)$$

where N_{CNT-u} is the number of atomic contacts of CNT(C) with urea and N_{CNT-w} is the numbers of atomic contacts of CNT(C) with water (W) molecules. If two molecules locate closer than 0.35 nm, they are in contact. The total number of urea atoms (M_u) and water atoms (M_w) were used to normalize $C_u - C_{CNT}$ values.⁴⁷

Results and Discussion

System equilibration

Equilibrium of system has been monitored by quantities such as the total and potential energy, the temperature and the pressure of the systems. Figures 1a and 1b show that the total energy of all simulated systems converge smoothly to a constant energy within 1.5 ns of the equilibration phase,

indicating that all systems can be used for subsequent data sampling.

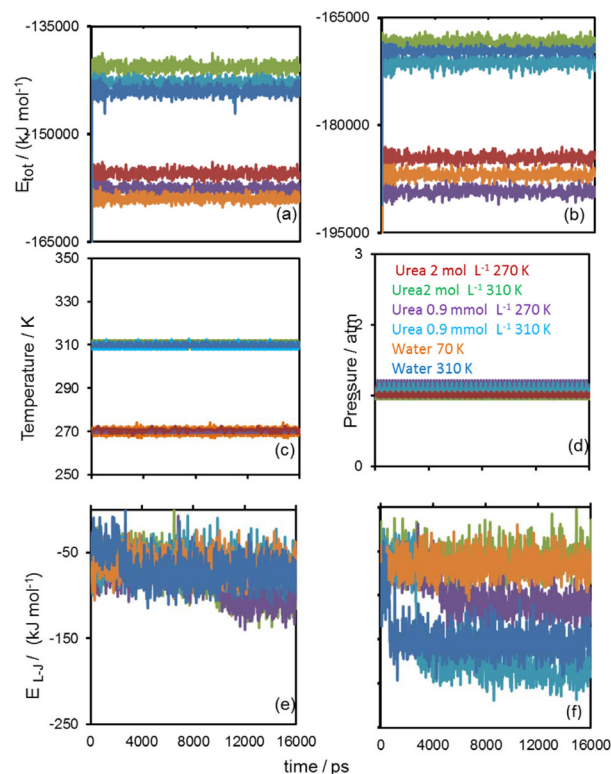


Figure 1. Total energy of (a) CNT (8, 5)-Tretinoin and (b) CNT (10, 7)-Tretinoin systems. Temperature (c) and pressure (d) of systems in CNT (10, 7). Lennard-Jones energy between (e) CNT (8, 5) and (f) CNT (10, 7) and Tretinoin as a function of simulation time (picosecond).

Figure 1a and 1b also exhibit that simulated systems at 270 K have a lower total energy compared to those simulated at 310 K because total energy increases with temperature.¹⁷ The comparison of water and urea total energies shows less total energy or more system stability in 0.9 mmol L⁻¹ urea. The stability can be due to the presence of urea in the system that decreases the impact and kick of water to other components of system, and enhances the system stability. Therefore, the movement of water and urea increases by temperature, so that instability and total energy of the system increase. Comparison of 0.9 mmol L⁻¹ and 2 mol L⁻¹ urea curves shows that system instability changes with urea concentrations. It also shows that the total energy of the larger tube is more negative due to less hindrance resulted from the movement of water, especially water permeation through the nanotube and therefore, stability increases. Figures 1c and 1d report the temperature and pressure curves of two systems as well as the steady state in these parameters that also confirms equilibrium in an ensemble with fixed number of atoms, pressure and temperature.

Table 2. Least squares fit for RMSD of CNT and Tretinoin

No.	lsq fit for Tretinoin / nm	lsq fit for CNT / nm	No.	lsq fit for Tretinoin / nm	lsq fit for CNT / nm
1	0.174718	0.0348593	7	0.115193	0.0307129
2	0.271554	0.0357247	8	0.294058	0.0381728
3	0.14807	0.0329469	9	0.186304	0.0387552
4	0.217506	0.0244822	10	0.186304	0.0387552
5	0.217568	0.0378001	11	0.252131	0.0380209
6	0.205459	0.0379217	12	0.172642	0.0381094

The L-J energy between Tretinoin and CNT (Figure 1e and 1f) reveals that the energy decreases in 0.9 mmol L^{-1} urea and water at 310 K and decreases in 2 mol L^{-1} urea (Figure 1f). The energy of the smaller tubes does not show any systematic trend (Figure 1e), but Figure 1f shows that the most stable condition between nanotubes-Tretinoin is at the normal level of urea (0.9 mmol L^{-1}) and the most unstable mode is in 2 mol L^{-1} urea. Assuming that the system has reached to an equilibrium state, we can compare the first and the final structure obtained in the simulation. Table 2 presents root mean square deviation (RMSD) of Tretinoin and CNT structures after least-squares (lsqs) fitting. Small values of lsq fit for Tretinoin and CNT indicate how much the structure differs.

The effect of CNT size

CNT (10, 7) and CNT (8, 5) (No. 2 and 8 from Table 1) were selected to examine how the size of nanotubes would affect Tretinoin-CNT interaction. The results showed that the Tretinoin did not insert into the CNT (8, 5) after 16 ns (Figure 2 top). However, the general preference of Tretinoin insertion can be observed in CNT (10, 7) through our simulations.

Figure 2 (middle) depicts the time-coursed snapshots of the Tretinoin-CNT (10, 7) frame. It indicates a fast insertion process of Tretinoin into the CNT. After optimization, the Tretinoin came near the tube and it began to enter the CNT.

It is very important to investigate the nature of interactions between CNT and the drug. In an aqueous environment, existence of CNT increases the hydrogen bonds at the water-CNT interface. Hydrogen atom of carbons attracts hydrogen or oxygen of the water and forms hydration shell outside and inside CNT surface.⁴⁸ This hydration shell may affect the absorption between CNT and other molecules.⁴⁹ Then, drug drives away the water molecules from CNT surface, and drug can assemble and absorb on the CNT surface to form a more favourable structure.⁵⁰ This effect is observed in both CNTs. Figure 2 (below) presents some of the water molecules entered

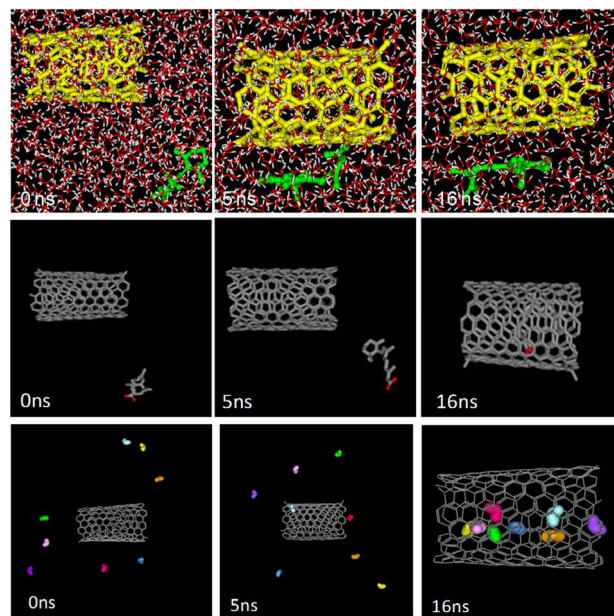


Figure 2. Time-course snapshot taken by DS Visualizer from Tretinoin interacting with CNT (8, 5) (top pictures), with CNT (10, 7) (middle pictures). Water flow into the CNT (10, 7) (movement of 8 randomly selected water molecules) (below pictures) during 16 nanosecond (ns) simulation time.

the CNT (10, 7) suggesting that water insertion into the nanotube can be a driving force to push the drug into the nanotube. In the case of Tretinoin, water molecules might make hydrophilic interactions with the polar chemical groups of Tretinoin. This hydrophilic force, provided by the water molecules inside the nanotube, might bring Tretinoin inside the CNT (10, 7). Maybe there is not enough water flow and hydrophilic force to encapsulate Tretinoin in CNT (8, 5). It means that the hydrophobic and the van der Waals interaction play vital role in drug-CNT interactions.

The results of L-J energy (Figure 3a) show no van der Waals interaction between the drug and the CNT (8, 5) until 5 ns, while a few weak interactions could be detected as Tretinoin moves forward the nanotube. By contrast, it exhibits significant van der Waals interaction between CNT (10, 7) and Tretinoin, leading Tretinoin enter the CNT (10, 7). It also confirms more van der

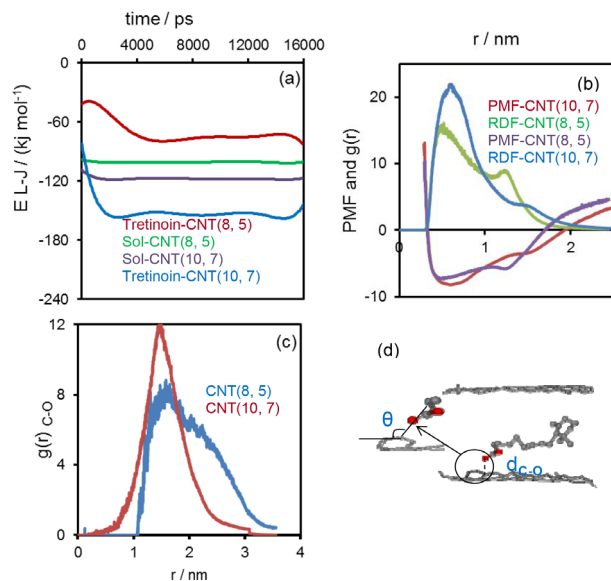


Figure 3. (a) L-J energy between CNT and Tretinoin or water molecules (at 310 K), (b) potential of mean force and RDF for Tretinoin-CNT (at 310 K), (c) distribution plot of the distances between C-O, where the dashed line represents the d_{C-O} from the B3LYP/6-31G optimization,¹⁷ (d) schematic representation of the distances from the CNT surface to the O atom of Tretinoin, d_{C-O} , and the estimated angle, θ , between the CNT vector from the O atom of Tretinoin.

Waals interaction energy of CNT (8, 5)-water than CNT (10, 7)-water; that might be due to the Tretinoin insertion into the CNT (10, 7) that decreases water interaction with CNT. It can be concluded that, although the water flow inside the nanotubes might act as a driving force for drug encapsulation inside the CNTs based on what have recently been observed,⁵¹ other factors such as the size of nanotube play an important role. To investigate the effect of tube size on the process of encapsulation, PMF is measured. Figure 3b displays the PMF profile along the CNT. The obtained profile shows that the PMF of CNT (10, 7) decreases when the drug is moving inside the tube and confirms the spontaneous encapsulation. When the Tretinoin reaches the CNT edge at 0.8 nm and 1.2 nm of CNT (10, 7) and CNT (8, 5) respectively, the PMF decreases. Then, it decreases rapidly by a reduction in the distance between drug and CNT, up to 0.4 nm. A flat region appears between 0.4 nm to 0.8 nm with one small local minimum for CNT (10, 7) and for CNT (8, 5). The flat region appears between 0.4 to 1.4 nm with some local minima. After 0.8 nm, the PMF tends to increase where the drug is going outside the nanotube. The relatively large barrier at the 0.4 nm and 0.8 nm indicates that the stable position of the drug is achieved in this flat region. RDF of Tretinoin-CNT is also compared in Figure 3b, and the intensity is more for CNT (10, 7).

The results revealed that the drug molecule stays inside the CNT cavity throughout the simulation time at 310 K in water, and that this was possibly due to lone pair of oxygen

atoms as donor atoms that can transfer electron to acceptor atoms σ^* or π^* in carbon nanotube, that is the most important common interaction in the nanotube-Tretinoin composite, as detected previously.^{17,26} Figure 3c plots the RDF diagram of tube surface to O atom of drug which reveals characteristic of this interaction. The narrow distribution with the most probable distances at 1.4 nm, together with a minimum and maximum variation of only 1 nm were found in the CNT (10, 7). The most probable angle, θ , between the vector lining from O atom of Tretinoin and the C-C vector of CNT from the parallel orientation to the inner surface of the CNT was 120° (refer schematic in Figure 3d for definition). The probable distances at 1.4 nm and the angle is in good agreement with the related distance and angle between the oxygen atom of Tretinoin and benzene rings of CNT obtained from the DFT approach using the B3LYP/6-31G level of theory.¹⁷ In the case of the systems containing CNT (8, 5), the most frequent probability for the location of C-O was within the 1.7 nm, and with a broader peak starting at the equivalent distance of 1 nm and ending at longer distance by > 2 nm. This suggests the reduced strength of π - π stacking interactions between Tretinoin molecules and the CNT (8, 5) surface. In other words, the results clearly demonstrated that the loading of Tretinoin molecules inside CNT (10, 7) increases the drug binding interaction to its transporter.

The effect of urea and temperature

This section compares the behavior of Tretinoin in water, 0.9 mmol L^{-1} and 2 mol L^{-1} urea. Figures 4a and 4b compare the strength of direct interactions between Tretinoin and tube and the inset pictures depict the related distance diagrams. The results of Figure 4a confirm more interaction of CNT-Tretinoin in water. In Figure 4b it can be seen that $g(r)$ intensity increases in 0.9 mmol L^{-1} urea that confirms distance results obtained in the inset curves of distance. Sharp peak in Figure 4b related to systems of water and 0.9 mmol L^{-1} urea shows more ordered Tretinoin near the CNT and confirms better solvation of the Tretinoin with time. All flat curves of this figure relate to weak interaction at lower temperatures. Furthermore, up to nearly 3000 ps, the distance between Tretinoin and CNT (10, 7) rapidly decreases in 0.9 mmol L^{-1} urea. Less distance was obtained between CNT-drug at higher temperatures and in 0.9 mmol L^{-1} urea and water and the maximum distance was observed in 2 mol L^{-1} urea. Figures 4c-4f compare the strength of direct interactions between urea or water and Tretinoin during the first (before the insertion) and the last 5 ns (after the insertion). In this figure, the magnitude of RDF is directly proportional to water insertion through CNT.

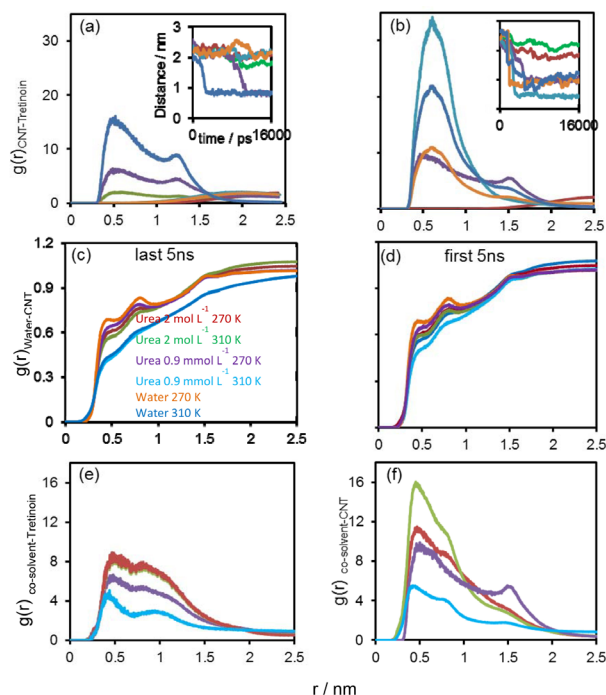


Figure 4. RDF of Tretinoin around (a) CNT (8, 5) and (b) CNT (10, 7). Inset (a) alteration of the center-of-mass distance of Tretinoin-CNT (8-5) and inset (b) CNT (10, 7). RDF between the water and CNT during (c) last and (d) first 5 ns of simulation in CNT (10, 7). RDF of urea around (e) Tretinoin and (f) around CNT.

Before the insertion (first 5 ns), there are more water molecules near the CNT in water than in urea, and there are not any special differences between curves of 270 K that no insertion has been reported. The result of interaction after the insertion (last 5 ns) indicates more water molecules near CNT in water and urea at 270 K that no insertion has been observed. Intensity of peak decreases in urea and water at 310 K, suggesting that insertion of Tretinoin into the CNT causes poor solvation of the CNT. Comparison of RDF in water and urea at 270 K reveals more water flow in the absence of urea due to lack of urea flow through the nanotube.

In conclusion, flow of water into CNT helps Tretinoin insertion at the beginning of the simulation and after insertion; drug molecule drives out or dries water molecules from the nanotube. On the other hand, the strength of the interaction between water and the CNT slightly increases with time. This finding shows that water solvated the CNT slightly better at the end of the simulation (last 5 ns), after insertion.

Figure 4e shows that RDF of urea around CNT decreases more in 0.9 mmol L⁻¹ urea at 310 K due to insertion of Tretinoin into the tube. The higher value of RDF for CNT (10, 7) in comparison with CNT (8, 5) at 270 K is due to the bigger size of the tube. These results are consistent with the results of Figure 4c and 4d. Existence

probability of urea around Tretinoin for (Figure 4f) CNT (8, 5) at 270 and 310 K is more than CNT (10, 7) at 310 K that no insertion is observed.

Figure 5 shows the number of solvent (water/urea) molecules inside the CNT during the course of the simulation.

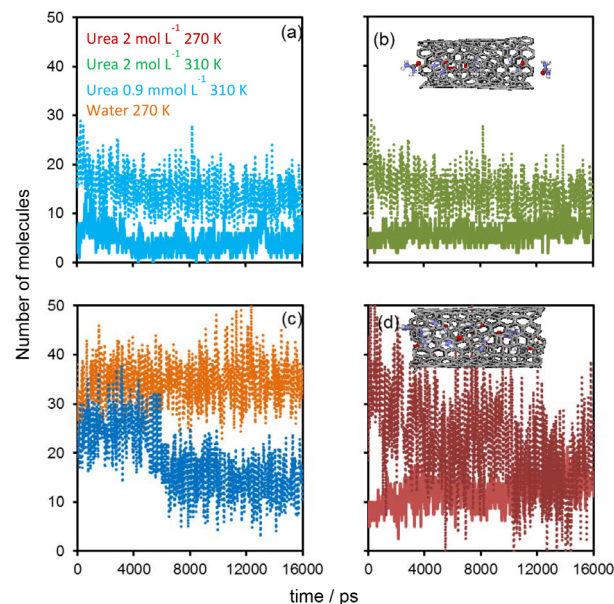


Figure 5. Number of urea (dashed lines) and water (solid lines) molecules within the CNT (10, 7) as a function of simulation time. Inset: snapshot of a “perfect” urea wire.

Figure 5a shows that the number of urea molecules inside the tube increases up to 2 ns, which indicates the formation of defect urea wires inside the tube and then the number of urea molecule decreases. This can be explained such that in 0.9 mmol L⁻¹ urea, the wire is not very stable and when the drug enters the tube, the number of urea molecules decreases. The dashed line curve shows that almost all water molecules inside the CNT are replaced by urea within the first 2 ns and water molecules inside the tube decrease. After 2 ns, the number of urea and water molecules decreases due to the encapsulation. Figure 5b corresponds to the 2 mol L⁻¹ urea, which indicates that the number of urea increases from the first nanoseconds and forms nearly perfect wires and due to wire formation, the number of water molecules decreases and the wire is strong enough to inhibit encapsulation. Comparison of Figure 5a and 5b shows that at low concentrations of urea, number of urea increases at first and then decreases, due to the phenomenon of the drug encapsulation occurring, whereas at high concentration of urea, wire formation is strong enough to inhibit encapsulation. According to the inset in Figure 5b, a “defective” and perfect urea wire are observed at low and high concentration of urea,

respectively.⁵² Figure 5c compares two temperatures and the result reveals the increase of water molecule at the beginning of optimization and after 6 ns, water inside the tube decreases due to the encapsulation of the drug inside the tube at 310 K. The curve of 270 K shows an inverse trend over time, the number of water molecules in the tube increases and reaches a nearly constant value. Results confirm that maybe the encapsulation of drug contributes to more water at higher temperatures. Figure 5d compares the number of water and urea in the 2 mol L⁻¹ urea at 270 K. Results show the number of urea molecules increases with time and replace water molecules. No encapsulation is observed in this case, and instead, we can view a perfect wire of urea. As shown in the inset of Figure 5d, urea has a robust ability to form uninterrupted molecular wire at high concentrations. However, this wire can be interrupted at low concentration due to stronger ability of encapsulation. Comparison of the Figure 5b and 5d represents more water molecules replaced by urea at higher temperature in 2 mol L⁻¹ urea.

Figure 6 focuses on the contact coefficient related to the number of 0.9 mmol L⁻¹ and 2 mol L⁻¹ urea molecules in contact with CNT.

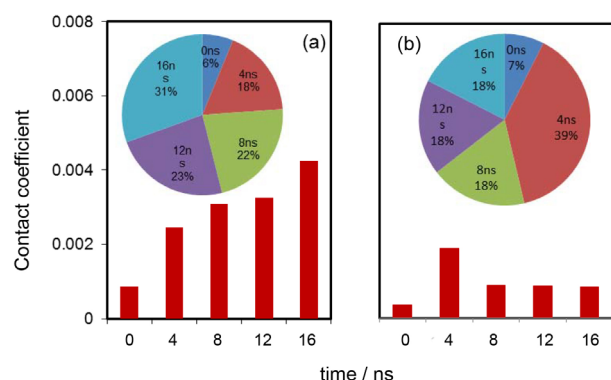


Figure 6. Contact coefficient of urea with CNT in (a) 2 mol L⁻¹ urea and (b) 0.9 mmol L⁻¹ urea at 310 K.

Figure 6a shows that the contact of urea-CNT increases during the time in 2 mol L⁻¹ urea, and Figure 6b indicates the contact ratio increases up to 4 ns and then decreases and reaches a constant value in 0.9 mmol L⁻¹ urea. The difference maybe due to the ability of the drug encapsulation at low concentration of urea that reduces urea contact with the tube.

Figures 7a and 7b present the profile of the PMF, and the positions of the minima are (0.3-1.3 nm) in 0.9 mmol L⁻¹ urea and (1.8-2.2 nm) in water and the depth of the minima increases in urea solutions and is deeper at higher temperature. The PMF decreases mainly when the drug reaches the tube edge and encapsulation occurs.

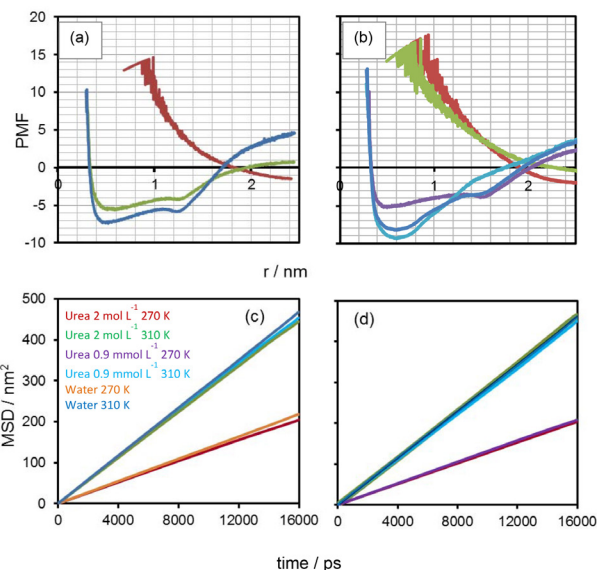


Figure 7. Comparisons of the PMF and MSD of Tretinoin in (a) and (c) CNT (8, 5) and (b) and (d) CNT (10, 7).

Figures 7c and 7d show the MSD of Tretinoin and it confirms less mean square displacement or transport processes of Tretinoin in the 0.9 mmol L⁻¹ urea and water solutions, respectively, and this is due to encapsulation process. Table 3 presents values of self-diffusion constant D_A . The slope of MSD is lower at 270 K, indicating that the D_A increases with temperature.

Table 3. Values of D_A for CNT (8, 5) and (10, 7)-water at 310 and 270 K

No.	D_A / (nm ² ps ⁻¹)	No.	D_A / (nm ² ps ⁻¹)
1	0.002267	7	0.002217
2	0.004867	8	0.004767
3	0.002183	9	0.002183
4	0.004751	10	0.004667
5	0.002133	11	0.002117
6	0.004667	12	0.004833

The results show that at low temperatures, in both sizes of the nanotube, maximum diffusion coefficient is in water, 0.9 mmol L⁻¹ and 2 mol L⁻¹ urea, respectively. The reason is that no encapsulation observed previously at 270 K and therefore, drug mobility or travel is higher in water and less in 2 mol L⁻¹ urea. The comparison of CNT (8, 5) at 310 K shows that the trend of diffusion change is similar to lower temperature, while in larger tube, the trend of the diffusion is: urea 2 mol L⁻¹ > water > urea 0.9 mmol L⁻¹. Higher diffusion of the drug in 2 mol L⁻¹ urea and lower diffusion in water and 0.9 mmol L⁻¹ urea maybe due to encapsulation.

Figure 8 shows time-coursed snapshot picture taken from the system No. 10 (Table 1) in the 0.9 mmol L⁻¹ urea

Table 4. Potential, kinetic and total energies and obtained heat capacity (C_p)

No.	Potential energy / (kJ mol ⁻¹)	Kinetic energy / (kJ mol ⁻¹)	Total energy / (kJ mol ⁻¹)	C_p / (kJ mol ⁻¹ K ⁻¹)
1	-187550	28575	-158975	898.0017
2	-177015	32948	-144067	1297.364
3	-183701	26061	-157640	812.0066
4	-173224	30347	-142877	1109.918
5	-186113	30632	-155481	872.5138
6	-175673	34987	-140686	1187.272
7	-224990	38097	-186893	647.015
8	-212128	42459	-169669	1616.907
9	-210377	21131	-189246	644.3662
10	-201920	30616	-171304	1116.798
11	-231017	46417	-184600	896.3365
12	-223571	55081	-168490	1840.182

before and after simulation. It shows that Tretinoin inserts into the CNT (10, 7) in urea.

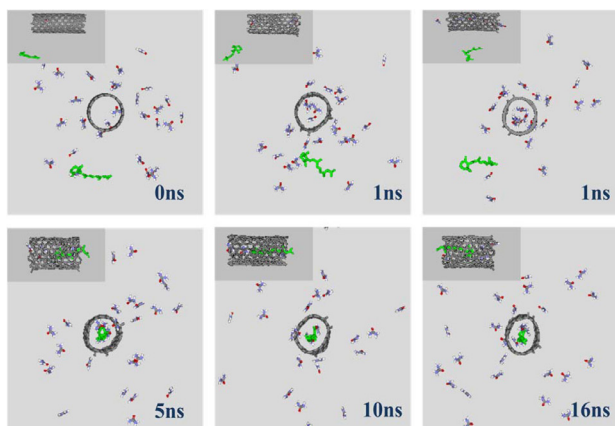
**Figure 8.** Snapshot picture of Tretinoin-CNT (10, 7) system in urea at 310 K before simulation, after position restrains (1 ns) and after 1 to 16 ns.

Table 4 presents potential, kinetic and total energies and heat capacity of all studied systems.

From this table, it is obvious that the kinetic energy and heat capacity increase with temperature of the system (Figure 1). This is due to the increase of thermal motions that make the structure less stable. The potential and total energy value for CNT (10, 7) is lower than the CNT (8, 5). The heat capacity decreases with CNT van der Waals radius and as a result, the system becomes more stable. By comparison of water, 0.9 mmol L⁻¹ and 2 mol L⁻¹ urea, it becomes clear that the total and potential energy and heat capacity of the system in 0.9 mmol L⁻¹ are lower than water and 2 mol L⁻¹ urea, respectively. So, stability of the system is higher in 0.9 mmol L⁻¹ urea.

One possible reason for the different behavior of water and urea is the difference of water/urea properties presented in Table 5.

Table 5. The dipole moment (μ), dielectric constant (ϵ) and molecular weight of water/urea⁵³

Solvent	Dipole moment / Debye	Dielectric constant / (F m ⁻¹)	Molecular weight / (g mol ⁻¹)
Urea	4.56	82.33	60
Water	1.85	80.10	18

A number of papers have shown LIE as a method with fast and reliable estimates of binding free energies.^{54,55} The electrostatic and van der Waals contributions to the free energy difference are given in Table 6. The contribution decomposition of free energy shows that the van der Waals term plays the most important role for stability of the CNT-Tretinoin system. The electrostatic term has a negative smaller contribution to the binding free energy.

When the drug is located outside CNT, the Gibbs free energy is less negative and rapidly decreases after the drug enters the CNT or after encapsulation. This result was in good agreement with those obtained from previous study.⁵⁶ According to previous study, negative free energy confirms that the drug prefers to locate inside the CNT.⁵⁶ The most negative value of free energy is in water and 0.9 mmol L⁻¹ urea at 310 K that is due to the observed encapsulation in these systems. Taking result of Table 5 and 6 altogether reveals that the Gibbs-free energy values of the interaction between Tretinoin and CNT molecules decrease with solvent dielectric constant. The binding free energies are less negative than those got by Johnson,⁵⁷ Wenping⁵⁰ and Garate *et al.*⁵⁸ Because CNT in this letter has a bigger diameter as compared to CNT (11, 0) and they have used different target molecules in their calculations.

Table 6. Free energy values of the systems obtained from LIE method

No.	Bound / (kJ mol ⁻¹)		Free / (kJ mol ⁻¹)		Free energy / (kJ mol ⁻¹)
	L-J	VDW	L-J	VDW	
1	-66.555	-478.31	-66.317	-478.51	-0.086
2	-89.867	-456.48	-59.764	-465.14	-13.666
3	-81.831	-470.74	-69.531	-474.83	-5.495
4	-61.931	-462.06	-62.173	-462.71	0.227
5	-65.766	-471.32	-68.854	-460.15	-0.243
6	-70.267	-475.17	-71.504	-461.23	-1.613
7	-66.473	-479.03	-66.317	-478.51	-0.160
8	-149.93	-435.27	-59.764	-465.14	-40.303
9	-98.685	-464.75	-69.531	-474.83	-14.885
10	-158.13	-434.63	-62.174	-462.71	-43.486
11	-70.824	-464.55	-68.180	-465.03	-1.242
12	-61.189	-464.312	-60.465	-463.76	-0.325

Conclusions

Molecular dynamics simulation sheds more light on to the influence of urea, temperature and CNT size on insertion of an anticancer drug, Tretinoin into CNT. Our results show that the proper diameters of the CNT and water flow are the important factors for the drug encapsulation. Results show that during insertion, drug pushes out water and urea molecules out of CNT. The hydrophilic force, provided by the water molecules inside the nanotube, might brings Tretinoin inside the CNT. Furthermore, decreased PMF profile followed by decreased distance of CNT-drug and their reduced free energy of interaction is accompanied by entering of the drug into the CNT. Heat capacity and energy results have revealed that the encapsulated form is much more stable at lower temperatures and in the normal concentration of urea. It can be concluded that addition of urea at the normal level can increase system stability and decreases heat capacity, however; excessive addition of urea makes the system unstable and shifts the heat capacity of the system toward positive amounts. In conclusion, according to the most negative Gibbs free energy, urea at the normal level is effective in placing Tretinoin into the CNT (10, 7). Since both Tretinoin and CNT contain conjugated aromatic rings and lone pair electrons, then π - π stacking interactions are expected to be established between the oxygen atom of Tretinoin and the CNT inner wall surface. In contrast, at high urea concentrations, drug does not encapsulate due to wire formation inside CNT. Taken altogether, the obtained data provide useful information toward the urea effect on insertion process.

Acknowledgements

The financial support of Damghan University and University of Tehran is acknowledged.

References

- Chen, Q.; Wang, Q.; Liu, Y. C.; Wu, T.; Kang, Y.; Moore, J. D.; Gubbins, K. E.; *J. Chem. Phys.* **2009**, *131*, 15101.
- Park, K.; *ACS Nano* **2013**, *7*, 7442.
- Pantarotto, D.; Briand, J. P.; Prato, M.; Bianco, A.; *Chem. Commun.* **2004**, *10*, 16.
- Pantarotto, D.; Singh, R.; McCarthy, D.; *Angew. Chem., Int. Ed.* **2004**, *43*, 5242.
- Bianco, A.; Kostarelos, K.; Prato, M.; *Curr. Opin. Chem. Biol.* **2005**, *9*, 674.
- Zhang, W.; Zhang, Z.; Zhang, Y.; *Nanoscale Res. Lett.* **2011**, *6*, 555.
- Wong, B. S.; Yoong, S. L.; Jagusiak, A.; Panczyk, T.; Ho, H. K.; Ang, W. H.; Pastorin, G.; *Adv. Drug Delivery Rev.* **2013**, *13*, 188.
- Liu, P.; *Ind. Eng. Chem. Res.* **2013**, *52*, 13517.
- Lin, J.; Eder, M.; Weinmann, S.; *Ann. Intern. Med.* **2011**, *154*, 190.
- Narayanan, D.; Saladi, R.; Fox, J.; *Int. J. Dermatol.* **2010**, *49*, 978.
- Sersa, G.; Miklavcic, D.; Cemazar, M.; Rudolf, Z.; Pucihar, G.; Snoj, M.; *Eur. J. Surg. Oncol.* **2008**, *34*, 232.
- Dhar, S.; Liu, Z.; Thomale, J.; Dai, H.; Lippard, S. J.; *J. Am. Chem. Soc.* **2008**, *130*, 11467.
- Albertorio, F.; Hughes, M. E.; Golovchenko, J. A.; Branton, D.; *Nanotechnology* **2009**, *20*, 395101.

14. Johnson, R. R.; Johnson, A. T. C.; Klein, M. L.; *Nano Lett.* **2008**, *8*, 69.
15. Jung, S.; *J. Am. Chem. Soc.* **2010**, *132*, 10964.
16. Zhao, X.; Johnson, J. K.; *J. Am. Chem. Soc.* **2007**, *129*, 10438.
17. Rungnim, C.; Arsawang, U.; Rungrotmongkol, T.; Hannongbua, S.; *Chem. Phys. Lett.* **2012**, *550*, 99.
18. Ascenso, A.; Cruz, M.; Euleterio, C.; Carvalho, F. A.; Santos, N. C.; Marques, H. C.; Simoes, S.; *J. Liposome Research* **2013**, *23*, 211.
19. Kofinger, J.; Hummer, G.; Dellago, C.; *Proc. Natl. Acad. Sci. U. S. A.* **2008**, *105*, 13218.
20. Hummer, G.; Rasaiah, J. C.; Noworyta J. P.; *Nature* **2001**, *414*, 188.
21. Kantamneni, H.; *Int. J. Eng. Res. Tech.* **2013**, *2*, 2278.
22. Dalili Mansour, N.; Zare, K.; Elsagh, A.; *J. Phys. Theor. Chem.* **2010**, *7*, 15.
23. Levin, E. J.; Quick, M.; Zhou, M.; *Nature* **2009**, *462*, 757.
24. Xiu, P.; Tu, Y.; Tian, X.; *Nanoscale* **2012**, *4*, 652.
25. Liu, Y.; Consta, S.; Goddard, W. A.; *J. Nanosci. Nanotechnol.* **2010**, *10*, 3834.
26. Hesabi, M.; Hesabi, M.; *J. Nanostruct. Chem.* **2013**, *3*, 22.
27. Wohlrab, W.; *Z. Hautkrankh.* **1990**, *65*, 803.
28. *HyperChem (TM) Professional 7.51*; Hypercube, Inc.: 1115 NW 4th Street, Gainesville, Florida, USA.
29. Dewar, M. J. S.; Zoebisch, E. G.; Healy, E. F.; Stewart, J. J. P.; *J. Am. Chem. Soc.* **1985**, *107*, 3902.
30. Schuttelkopf, A. W.; van Aalten, D. M. F.; *Acta Crystallogr.* **2004**, *60*, 1355.
31. <http://turin.nss.udel.edu/research/tubegenonline.html>, accessed in October 2014.
32. Ricci, C. G.; de Andrade, A. S.; Mottin, M.; Netz, P. A.; *J. Phys. Chem. B.* **2010**, *5*, 9882.
33. Bussi, G.; Donadio, D.; Parrinello, M.; *J. Chem. Phys.* **2007**, *126*, 14101.
34. Fincham, D.; *Mol. Simul.* **1992**, *8*, 165.
35. Gao, H.; *Nano Lett.* **2003**, *3*, 471.
36. Yakubovich, A. V.; Solovyov, I. A.; Solovyova, A. V.; Greiner, W.; *J. Eur. Phys. D* **2009**, *51*, 25.
37. <http://manual.gromacs.org/programs/gmx-energy.html>, accessed in October 2014.
38. Allen, M. P.; Tildesley, D. J.; *Computer Simulations of Liquids*, Oxford Science Publications: Oxford, 1987.
39. Qvist, A.; Medina, C.; Samuelsson, J.; *Protein Eng.* **1994**, *7*, 385.
40. Wang, W.; Wang, J.; Kollman, P. A.; *Proteins* **1999**, *34*, 395.
41. Almlof, M.; Brandsdal, B. O.; Aqvist, J.; *J. Comput. Chem.* **2004**, *25*, 1242.
42. Sanguinetti, M. C.; Jiang, C. G.; Curran, M. E.; Keating, M. T.; *Cell* **1995**, *81*, 299.
43. Osterberg, F.; Aqvist, J.; *FEBS Lett.* **2005**, *579*, 2939.
44. Hansson, T.; Marelus, J.; Aqvist, J.; *J. Comput. Aided Mol. Des.* **1998**, *12*, 27.
45. Diaz, L.; Bujons, J.; Delgado, A.; Gutierrez-de-Teran, H.; Aqvist, J.; *J. Chem. Inf. Model.* **2011**, *51*, 601.
46. O'Brien, E. P.; Dima, R. I.; Brooks, B.; Thirumalai, D.; *J. Am. Chem. Soc.* **2007**, *129*, 7346.
47. Hilder, T. A.; Gordon, D.; Chung, S. H.; *Nanomed: Nanotechnol. Biol. Med.* **2011**, *7*, 702.
48. Gordillo, M. C.; Marti, J.; *Phys. Rev. B: Condens. Matter Mater. Phys.* **2008**, *78*, 075432.
49. Shen, J. W.; Wu, T.; Wang, Q.; Kang, Y.; Chen, K.; *ChemPhysChem* **2009**, *10*, 1260.
50. Wenping, L.; *Chem. Phys. Lett.* **2011**, *514*, 311.
51. Torrie, G. M.; Valleau, J. P.; *J. Comput. Phys.* **1977**, *23*, 187.
52. Wan, R. Z.; Lu, H. J.; Li, J. Y.; *Phys. Chem. Chem. Phys.* **2009**, *11*, 9898.
53. Rauf, M. A.; Hisaindee, S.; Graham, J. P.; Nawaz, M.; *J. Mol. Liq.* **2012**, *168*, 102.
54. Nome, R. A.; *J. Braz. Chem. Soc.* **2010**, *21*, 2189.
55. Tan, J. J.; Kong, R.; Wang, C. X.; Chen, W. Z.; *J. Mol. Struct.: THEOCHEM* **2004**, *682*, 9.
56. Arsawanga, U.; Saengsawangb, O.; Rungrotmongkol, K.; Sornmee, P.; Wittayanarakul, K.; Remsungnend, T.; Hannongbuab, S.; *J. Mol. Graph. Model.* **2011**, *29*, 591.
57. Johnson, R. R.; Johnson, A. T. C.; Klein, M. L.; *Small* **2010**, *6*, 31.
58. Garate, J. A.; Perez-Acle, T.; Oostenbrink, C.; *Phys. Chem. Chem. Phys.* **2014**, *16*, 5119.

Submitted: July 20, 2014

Published online: October 17, 2014